Reactive Oxygen Species Are Involved in Plant Defense against a Gall Midge[C][W][OA]

Xuming Liu, Christie E. Williams, Jill A. Nemacheck, Haiyan Wang, Subhashree Subramanyam, Cheng Zheng, and Ming-Shun Chen*

Department of Entomology (X.L., M.-S.C.), Department of Statistics (H.W.), and United States Department of Agriculture-Agricultural Research Service Plant Science and Entomology Research Unit (M.-S.C.), Kansas State University, Manhattan, Kansas 66506; and United States Department of Agriculture-Agricultural Research Service Crop Production and Pest Control Research Unit and Department of Entomology (C.E.W., J.A.N.), Department of Biological Sciences (S.S.), and Department of Statistics (C.Z.), Purdue University, West Lafayette, Indiana 47907

Reactive oxygen species (ROS) play a major role in plant defense against pathogens, but evidence for their role in defense against insects is still preliminary and inconsistent. In this study, we examined the potential role of ROS in defense of wheat (*Triticum aestivum*) and rice (*Oryza sativa*) against Hessian fly (*Mayetiola destructor*) larvae. Rapid and prolonged accumulation of hydrogen peroxide (H_2O_2) was detected in wheat plants at the attack site during incompatible interactions. Increased accumulation of both H_2O_2 and superoxide was detected in rice plants during nonhost interactions with the larvae. No increase in accumulation of either H_2O_2 or superoxide was observed in wheat plants during compatible interactions. A global analysis revealed changes in the abundances of 250 wheat transcripts and 320 rice transcripts encoding proteins potentially involved in ROS homeostasis. A large number of transcripts encoded class III peroxidases that increased in abundance during both incompatible and nonhost interactions, whereas the levels of these transcripts decreased in susceptible wheat during compatible interactions. The higher levels of class III peroxidase transcripts were associated with elevated enzymatic activity of peroxidases at the attack site in plants during incompatible and nonhost interactions. Overall, our data indicate that class III peroxidases may play a role in ROS generation in resistant wheat and nonhost rice plants during response to Hessian fly attacks.

Reactive oxygen species (ROS) play a central role in plant defense against various pathogens (Mittler et al., 2004). Superoxide anion (O_2^-), hydrogen peroxide (H_2O_2), and hydroxyl radical are the three major forms of ROS. These molecules are highly reactive and toxic and can lead to the oxidative destruction of cells (Asada and Takahashi, 1987). The rapid accumulation of plant ROS at the pathogen attack site, a phenomenon called oxidative burst, is toxic to pathogens directly (Lamb and Dixon, 1997) and can lead to a hypersensitive response (HR) that results in a zone of host cell death, which prevents further spread of biotrophic pathogens (Heath, 2000; Gechev et al., 2006). In addition to the described direct effects, ROS can also serve as signals that lead to the activation of other defense mechanisms (Dat et al., 2000; Grant and Loake, 2000). Several mechanisms have been proposed for ROS generation in plants (Wojtaszek, 1997). Of these mechanisms, the NADPH-dependent oxidase system has received the most attention because of its similarity to the mammalian oxidase system that initiates ROS production in phagocytes and B lymphocytes as a response to pathogen attack (Apel and Hirt, 2004). In mammalian cells, NADPH-dependent oxidases catalyze the one-electron reduction of molecular oxygen to form O_2^-, which then undergoes dismutation to form H_2O_2 either spontaneously or catalyzed by superoxide dismutases. In plants, NADPH-dependent oxidases are also linked with O_2^- production in response to pathogen attack (Sagi and Fluhr, 2001) and wounding (Razem and Bernards, 2003). Insertion mutations of two Arabidopsis (*Arabidopsis thaliana*) NADPH-dependent oxidase subunit genes, *AtrbohD* and *AtrbohF*, largely eliminate ROS production during disease resistance reactions to avirulent pathogens (Torres et al., 2002).

In addition to NADPH-dependent oxidases, other classes of oxidases may also play a role in ROS generation (Mittler et al., 2004). Germin-like oxalate oxidases generate H_2O_2 from oxygen and oxalic acid

* Corresponding author; e-mail ming-shun.chen@ars.usda.gov.

The author responsible for distribution of materials integral to the findings presented in this article in accordance with the policy described in the Instructions for Authors (www.plantphysiol.org) is: Ming-Shun Chen (ming-shun.chen@ars.usda.gov).

[C] Some figures in this article are displayed in color online but in black and white in the print edition.

[W] The online version of this article contains Web-only data.

[OA] Open Access articles can be viewed online without a subscription.

www.plantphysiol.org/cgi/doi/10.1104/pp.109.150656

(Hu et al., 2003). Amine oxidases release H_2O_2 by oxidizing various forms of amines (Walters, 2003). NADPH oxidase-like alternative oxidases and glycolate oxidases have been suggested as producers of ROS as well (Apel and Hirt, 2004; Mittler et al., 2004). In addition to oxidases, pH-dependent cell wall peroxidases (members of the plant-specific, class III peroxidase superfamily; Passardi et al., 2004a) may also play a role in ROS generation in response to pathogen attacks under certain conditions (Lamb and Dixon, 1997; Bolwell et al., 2002; Mika et al., 2004).

The accumulation of plant ROS during defense is biphasic, with a rapid but weak transient accumulation (phase I) and a second, massive, and prolonged accumulation (phase II; Lamb and Dixon, 1997; Grant and Loake, 2000). The first phase of ROS accumulation is associated with infection of plants by either virulent or avirulent pathogens and is likely independent of de novo synthesis of ROS-generating enzymes. The second phase of ROS accumulation, however, is associated only with infection by avirulent pathogens and is an induced response dependent on the increased transcription of mRNA encoding ROS-generating enzymes. Because of its role in ROS generation, the level of NADPH-dependent oxidase transcript is often used as an indicator of oxidative defense, and the enzymatic inhibitor of oxidases, diphenylene iodonium, is widely used for ROS-related studies (Lamb and Dixon, 1997). In addition to the genes involved in ROS generation, the transcript levels of genes involved in ROS scavenging increase to limit ROS damage to host cells. Major ROS-scavenging enzymes include catalase, superoxide dismutase, ascorbate peroxidase, glutathione peroxidase, peroxiredoxin, thioredoxin, glutaredoxin, glutathione reductase, and dehydroascorbate reductase (Mittler et al., 2004).

The role of ROS in plant defense against insect herbivores is not clear. Lesions similar to HR symptoms have been observed in plants attacked by some insects (Chen, 2008). For example, HR-like lesions were observed in willow (*Salix viminalis*) tree varieties with resistance to the gall midge *Dasineura marginemtorquens* (Hoglund et al., 2005). HR-like symptoms were also observed with wheat (*Triticum aestivum*) resistance to the Hessian fly *Mayetiola destructor* (Grover, 1995), rice (*Oryza sativa*) resistance to the Asian rice gall midge *Orseolia oryzae* (Bentur and Kalode, 1996), peach (*Prunus persica*) resistance to the aphid *Myzus persicae* (Sauge et al., 1998), and bean (*Phaseolus vulgaris*) resistance to the bean-pod weevil *Apion godmani* (Garza et al., 2001). Despite these phenotypic observations, the biological significance of ROS in plant defense against insects remains to be established, and the mechanism for ROS generation in plants upon insect attack has yet to be determined. The activity of NADPH-dependent oxidases and the increase in H_2O_2 concentration in resistant plants following Russian wheat aphid (*Diuraphis noxia*) infestation (Moloi and van der Westhuizen, 2006) suggest that NADPH-dependent oxidases are involved in ROS generation in plants as a response to insect attack. However, mRNA levels of a NADPH-dependent oxidase and several genes encoding ROS-scavenging enzymes were not significantly altered in resistant wheat seedlings in response to Hessian fly attack, indicating that either ROS levels do not increase or an alternative mechanism for ROS generation is active following Hessian fly attack (Giovanini et al., 2006).

Hessian fly is a member of the gall midge family (Cecidomyiidae), and its interactions with wheat are considered a model system for the study of plant-gall midge interactions (Harris et al., 2003; Stuart et al., 2008). The Hessian fly-wheat interactions fit a typical gene-for-gene model in which the product of a dominant plant *R* gene mediates the induction of plant defenses through recognition of a corresponding avirulence gene product from the pathogen or insect (Flor, 1946). During incompatible interactions (wheat infested with avirulent larvae), resistant plants defend themselves effectively against Hessian fly larval attack and grow normally after some initial growth deficit (Anderson and Harris, 2006). As a result of plant defense, Hessian fly larvae die within 3 to 5 d after the initial attack. The exact cause for the larval death in resistant plants is not well understood. An increase in levels of transcripts and, in some cases, encoded proteins of many defense-related genes such as those encoding digestive enzyme inhibitors (Wu et al., 2008), lectins (Williams et al., 2002; Subramanyam et al., 2006, 2008; Giovanini et al., 2007), and enzymes for the biosynthesis of secondary metabolites (Liu et al., 2007) indicates that a combination of defense chemicals may be involved in resistance to Hessian fly. During compatible interactions (wheat infested with virulent larvae), susceptible plants are manipulated by Hessian fly larvae, including the suppression of plant defense (Sardesai et al., 2005; Saltzmann et al., 2010) and the reprogramming of plant metabolic pathways to create a nutrition zone for larval development (Puthoff et al., 2005; Harris et al., 2006; Liu et al., 2007; Saltzmann et al., 2008; Zhu et al., 2008). The manipulation of plants by Hessian fly larvae is likely achieved through salivary secretions (Chen et al., 2004, 2008), which may also trigger plant defense if recognized by the plant surveillance system (Garcia-Brugger et al., 2006). Wheat is the preferred host for the Hessian fly (Zeiss et al., 1993), but larvae can also live on barley (*Hordeum vulgare*) and other wheat-related species, although larval growth is slow and mortality is high (Harris et al., 2001). Rice is a nonhost for the Hessian fly (Chen et al., 2009b).

The objective of this research was to further clarify if ROS is involved in plant defense against Hessian fly attack. We observed a rapid elevation of ROS specifically in resistant wheat and nonhost rice plants attacked by Hessian fly larvae. Global analyses of gene transcripts known to be or potentially involved in ROS homeostasis indicated that class III peroxidases and oxalate oxidases, instead of NADPH-dependent

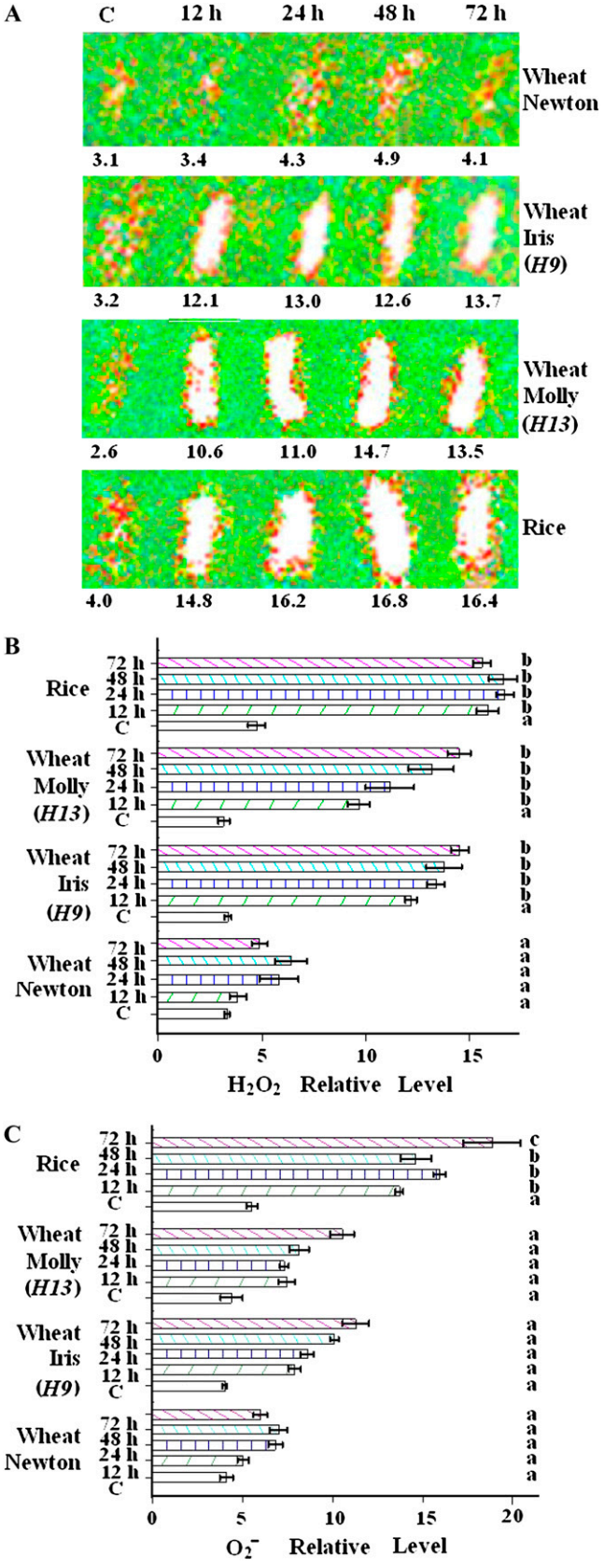

Figure 1. ROS accumulation in apoplasm. A, Representative fluorescence images of leaf sheaths at the larval attack sites stained for the presence of H_2O_2. Images were derived from nonattacked plants (C) and plants at 12, 24, 48, and 72 h after the initial attack by biotype L Hessian fly larvae. The dimensions of the H_2O_2-containing zones varied due to variations in larval densities and differences in larval migration. Each leaf sheath hosted 16 to 20 larvae. Relative fluorescence units are given below each image. Newton is a susceptible line containing no resistance gene. Iris contains R gene *H9*. Molly contains R gene *H13*. Rice is a nonhost. B, Average relative fluorescence obtained from images (similar to those shown in A) stained for H_2O_2 content. Each average value was derived from three biological replicates, with each replicate including readings from four lesions. C, Average relative fluorescence obtained from images stained for O_2^- content. The same numbers of leaf sheaths as in B were used.

oxidases, were likely the source of ROS generation in wheat plants during incompatible interactions.

RESULTS

Hessian Fly Induces Accumulation of ROS in Plants during Incompatible and Nonhost Interactions

Levels of apoplastic H_2O_2 at the larval attack site in plants during compatible, incompatible, and nonhost interactions were investigated via an uptake assay (see "Materials and Methods"). No significant change was detected in the level of fluorescence in wheat plants attacked by virulent larvae (Fig. 1A, Newton). In contrast, elevated fluorescence was observed at the attack sites of wheat plants hosting avirulent larvae [Fig. 1A, Iris (*H9*) and Molly (*H13*)] and on attacked rice plants (Fig. 1A, Rice), indicating that the levels of apoplastic H_2O_2 increased rapidly and stayed elevated for at least 72 h during incompatible and nonhost interactions. Semiquantitative analysis of luminescence images revealed an average 2- to 4-fold increase in apoplastic H_2O_2 concentration from plants during incompatible and nonhost interactions compared with nonattacked control plants [Fig. 1B, Iris (*H9*), Molly (*H13*), and Rice]. Although the fluorescence-based method is sensitive to increases in H_2O_2 accumulation, the signal intensity of images apparently reaches saturation when H_2O_2 reaches a certain concentration, as seen in Figure 1A. Therefore, the actual apoplastic H_2O_2 concentrations could be higher in some of the samples because the relationship between H_2O_2 concentrations and the intensities of fluorescent images is nonlinear at higher H_2O_2 concentrations.

Accumulation of O_2^- at the larval attack site was assayed with a similar method using a luminescence-based kit, yielding a different result from the accumulation of H_2O_2. No significant differences in O_2^- levels were detected between nonattacked control and attacked wheat during either compatible or incompatible interactions [Fig. 1C, Newton, Iris (*H9*), and Molly (*H13*)]. However, a strong increase in O_2^- content was detected in attacked rice during nonhost interactions (Fig. 1C, Rice).

Levels of cytosolic H_2O_2 were determined using a penetration assay (see "Materials and Methods"; Fig.

2). The overall pattern of cytosolic H_2O_2 changes was similar to that of apoplastic H_2O_2 changes, but the percentage increase in cytosolic H_2O_2 was less than that in apoplastic H_2O_2 during incompatible and nonhost interactions. Specifically, no significant changes were observed in the levels of fluorescence between control and attacked plants during compatible interactions at 48 h after initial larval attack. In comparison, there was a 30% to 40% increase in the levels of fluorescence in plants during incompatible and nonhost interactions.

H_2O_2 in Artificial Diet Is Lethal to Insects

Because Hessian fly larvae require live plant hosts and cannot be reared on an artificial diet, larval mortality due to ROS cannot be determined through feeding experiments. As an alternative, H_2O_2 was incorporated into an artificial diet and tested for toxicity to the larvae of *Drosophila melanogaster*, which belongs to the same order (Diptera) as the Hessian fly. As shown in Figure 3, H_2O_2 was highly toxic to *Drosophila* larvae, with a dose causing 50% lethality (LD50) of less than 0.05 μg mL^{-1}, or 1.7 μM in the diet.

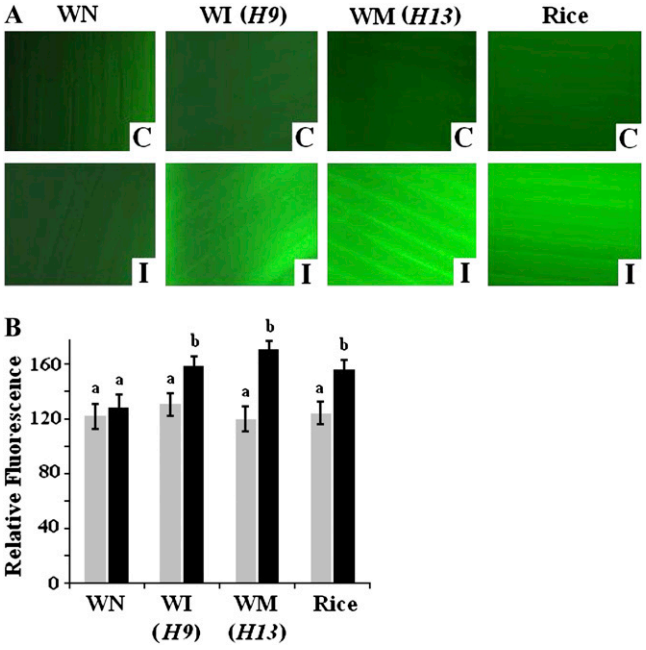

Figure 2. ROS accumulation in cytosol. A, Representative fluorescence images of leaf sheath cells at the larval attack site stained for H_2O_2. ROS were assayed with tissues from control (C) and attacked (I) plants at 48 h (see "Materials and Methods"). WN, WI (*H9*), and WM (*H13*) represent wheat Newton, wheat Iris (containing *H9*), and wheat Molly (containing *H13*), respectively. Light stripes are cell walls between cells. The images were obtained from a fluorescent microscope with amplifications 10 × 63. B, Average values of three biological replicates from control plants (gray bars) and plants attacked by Hessian fly (black bars). The letters a and b represent two groups that are statistically different ($P = 0.05$).

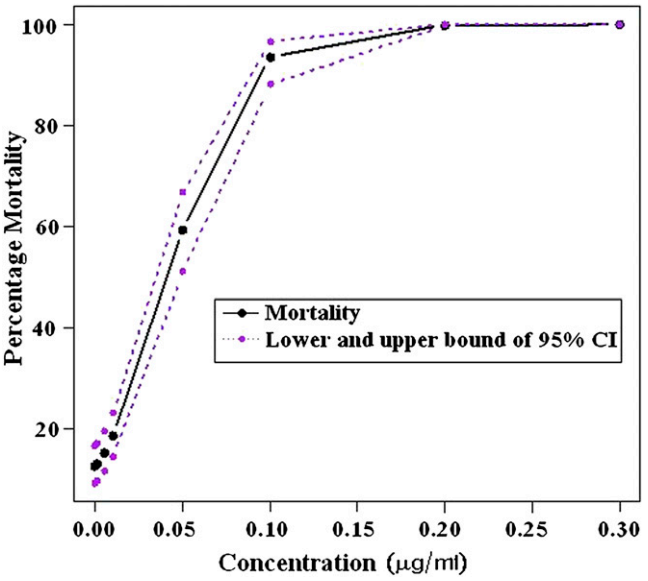

Figure 3. Toxicity of H_2O_2 to *Drosophila* larvae. The solid line represents the percentage of larval mortality at increasing concentrations of H_2O_2 on artificial diet. The dashed lines above and below the solid line represent upper and lower bounds of the 95% confidence interval (CI). LD50 is less than 0.5 μg mL^{-1} or 1.7 μM. [See online article for color version of this figure.]

Effect of Hessian Fly Attacks on Abundance of ROS Homeostasis Transcripts in Wheat

To gain insight into pathways contributing to ROS accumulation in resistant wheat during Hessian fly larval attack, microarray data were analyzed (Table I; Supplemental Table S1). A total of 250 probe sets were included in the analysis, 129 from genes classified as potential ROS generating and 121 from ROS-scavenging genes. Although the microarray samples covered the first 8 d of the interactions, Hessian fly attack led to changes in the levels of ROS homeostasis transcripts in resistant wheat during the first 72 h of incompatible interactions (Supplemental Table S1), after which ROS-related transcript levels returned rapidly to equal the control. Of the 129 ROS-generating genes corresponding to probe sets on the microarray, 43 (33.3%) encoded transcripts that increased in abundance by 24 h after attack and 30 (23.3%) were still elevated at 72 h in resistant plants, compared with controls at the same time points. Transcripts encoding NADPH-dependent oxidase, which is believed to be involved in the classic oxidative burst, did not change in abundance in resistant plants. Genes with the highest control transcript abundance (Supplemental Table S1 [SIC, signal intensity of control]) and the largest fold increase (or net increase) were members of the class III peroxidases (Table II; Supplemental Table S1). Only two transcripts corresponding to ROS-generating genes, glycolate oxidase and phospholipase A2, decreased in abundance in resistant plants (Table I; Supplemental Table S1). Of the 121 ROS-scavenging genes corresponding to probe

Table I. *Wheat microarray changes in transcript abundance following Hessian fly larval attack*

Gene Category[a]	Total Probe Sets[b]	Increased Abundance[c]		Decreased Abundance	
		R[d]	S[d]	R	S
Potential ROS generating	129	45	39	2	52
NADPH-dependent oxidases	3	0	1	0	0
Alternative oxidases	8	2	5	0	0
Glycolate oxidases	4	0	1	1	0
Oxalate oxidases	13	7	0	0	2
Amine oxidases	11	1	6	0	1
Class III peroxidases	83	34	22	0	45
Phospholipases A2	5	0	2	1	4
Xanthine dehydrogenases	2	1	2	0	0
Potential ROS scavenging	121	10	48	26	22
Catalases	6	0	5	0	0
Superoxide dismutases	4	0	4	0	0
Glutathione reductases	4	0	2	0	1
Dehydroascorbate reductases	4	0	1	1	1
Peroxiredoxins and thioredoxins	51	0	19	10	6
Glutaredoxins	15	5	2	0	4
Ferredoxins	14	0	4	9	9
Ascorbate peroxidases	12	2	7	3	1
Glutathione peroxidases	7	1	3	3	0
Flavanone 3-hydroxylases	4	2	1	0	0

[a]Gene category based on probe set annotation. [b]Number of probe sets on Wheat GeneChip microarray. [c]Transcript abundance level compared with level in a nonattacked control plant at the same time point, cumulative for all time points. [d]R, Resistant plants; S, susceptible plants.

sets on the microarray, nine (7.4%) encoded transcripts that increased in abundance by 24 h and five (4.1%) remained elevated 72 h after attack, whereas 22 (18.2%) decreased in abundance by 24 h and 11 (9.1%) remained low 72 h after attack (Table I; Supplemental Table S1) in resistant plants compared with controls at the same time points. The majority of transcripts in resistant plants corresponding to ROS homeostasis genes represented on the microarray did not change in abundance in response to Hessian fly larval attack.

Examination of microarray data from susceptible plants gave insight into ROS-related pathways that were manipulated by virulent Hessian fly larvae during compatible interactions. The same 250 probe sets were included in the analysis (Table I; Supplemental Table S1). Unlike the short-duration early response seen in incompatible interactions, changes in transcript abundance tended to begin later (20 transcripts showed their first sign of increase and 40 showed their first sign of decrease at 72 h after attack). In addition, many increases or decreases in transcript abundance were evident into the 8th d of the experiment during second-instar Hessian fly larval attack of susceptible plants. Of the 129 ROS-generating genes, 25 (19.4%) encoded transcripts that increased in abundance by 24 h after attack and 18 (14.0%) were still elevated at 192 h in susceptible plants, compared with controls at the same time points. By 24 h, six (4.7%) transcripts had decreased in abundance, and this number grew to 52 (40.3%) transcripts by 192 h. Of the 121 ROS-scavenging genes, 23 (19.0%) encoded transcripts that increased in abundance by 24 h after attack and 43 (35.5%) remained high after 192 h, whereas six (5.0%) decreased in abundance by 24 h and 13 (10.7%) were less abundant by 192 h. Compared with resistant plants, more defensive ROS-generating transcripts decreased and more ROS-scavenging transcripts increased in abundance in susceptible plants, especially at later time points. The response was rapid and short in resistant plants, but the response in susceptible plants continued throughout the experiment, which terminated on day 8 of larval attack.

In summary, increased abundance of the NADPH-dependent oxidase and glycolate oxidase transcripts detected in this experiment appeared to occur only in response of wheat to virulent larvae (compatible interaction). The oxalate oxidases were the only category of transcripts involved in ROS generation that became more abundant exclusively in resistant plants interacting with avirulent larvae. If class III peroxidase transcript levels responded, they tended to decrease in abundance in susceptible wheat and increase in resistant plants.

Effect of Hessian Fly Attacks on the Abundance of Transcripts Involved in ROS Homeostasis in Rice

To determine similarities between the Hessian fly-induced ROS-related gene responses in resistant wheat and the responses in nonhost rice, RiceChip microarray data were compared with the WheatChip

Table II. *Subset of potential ROS-generating genes with transcripts increasing in abundance in resistant wheat*

Includes transcripts from resistant plants fulfilling both criteria: (1) significant fold change of $P < 0.05$ in resistant plants compared with nonattacked plants, and (2) transcripts that did not increase in abundance in susceptible plants. NC, No change.

Wheat cDNA Identifier[a]	Fold Change[b]		Net Increase[c]	
	24 h	72 h	24 h	72 h
Oxalate oxidase[d]				
M21962	3.4	2.2	172.7	1,176.8
CA662687	1.5	NC	52.6	0
CA667447	2.3	2.8	123.9	428.9
CD373670	2.5	2.2	34.5	275.0
CA662341	1.8	2.3	25.1	284.8
Y09916	2.9	1.7	40.7	88.3
CA660893	2.1	1.8	28.2	145.4
Class III peroxidase[d]				
CK200808	12.1	2.7	889.8	959.2
BG606752	10.9	2.2	796.9	202.8
X85227	2.8	1.8	259.4	308.6
CK196925	2.7	1.8	137.7	88.1
CD454043	2.0	1.9	200.5	389.2
CK198851	1.8	1.7	270.1	1,402.2
CA612157	1.6	1.5	159.2	693.4
CK195044	1.6	1.3	84.1	47.8
CK193042	1.5	1.3	248.5	342.4
BQ838672	1.4	1.4	163.1	138.4
CD373872	1.3	1.4	220.5	232.2
CA685359	5.9	NC	149.0	0
CD373657	3.4	NC	92.6	0
BJ284138	2.1	NC	467.2	0
CA723231	2.2	NC	173.7	0
CD373595	1.5	NC	560.0	0
X16081	1.5	NC	143.0	0
CA697761	1.4	NC	148.4	0
CA714005	1.4	NC	335.1	0

[a]GenBank accession numbers corresponding to probe set sequences on the WheatChip. [b]Fold change is based on values for the same probe sets in nonattacked control plants at the same time point. [c]Net increase in fluorescence intensity is based on values for the same probe sets at the same time point in nonattacked control plants (SIC in Supplemental Table S1). Transcripts with the highest numbers are the most abundant. [d]Based on HarvEST and National Center for Biotechnology Information database searches.

data (Table III; Supplemental Table S1). Two minor differences in the design of the wheat and rice experiments were (1) the time points in the rice microarray analysis started 12 h earlier and spanned a shorter period (12, 24, 48, and 72 h after the initial Hessian fly larval attack) than those in the wheat analysis, and (2) transcript abundance in attacked rice plants was compared with a single control, unattacked plants that were harvested at the 12-h time point, rather than a control at each time point. The rice microarray contained probe sets representing 179 unique ROS-generating genes and 141 ROS-scavenging genes. As in resistant wheat, the ROS-generating response of rice appeared to initiate and terminate rapidly at the level of mRNA, with many transcript levels returning to control levels by 72 h. Of the 179 ROS-generating genes, 26 (14.5%) encoded transcripts that increased in abundance by 12 h after attack and 12 (6.7%) were still elevated at 72 h, compared with controls at the 12-h time point. Similar to the response in wheat, the rice NADPH-dependent oxidase transcripts, generally associated with oxidative burst, were not elevated compared with the control (with the exception of one of the eight rice transcripts having a maximum of a 2-fold increase). Also similar to the results for wheat, rice genes with the highest control transcript abundance (Supplemental Table S1, SIC) and the largest fold increase (or net increase) were members of the class III peroxidases (Table IV; Supplemental Table S1). Of the 141 ROS-scavenging genes, seven (5.0%) encoded transcripts that increased in abundance by 12 h and one (0.7%) remained elevated 72 h after attack, whereas 13 (9.2%) decreased in abundance by 12 h and one (0.7%) remained low 72 h after attack (Table III; Supplemental Table S1) compared with controls at the 12 h time point. The abundance of most of these 141 transcripts was not affected by Hessian fly attack, which was similar to the situation observed in resistant wheat. In both resistant wheat and nonhost rice, the transcript response to Hessian fly was rapid and short-lived, with genes belonging to the class III peroxidase category showing the greatest increase in transcript abundance (Tables II and IV), and the category with the greatest decrease was peroxiredoxins and thioredoxins (Supplemental Table S1).

Quantitative Reverse Transcription-PCR Analysis of Representative Transcripts

To validate changes observed in microarray analyses, primers covering 10 wheat and 13 rice transcripts (Supplemental Table S2) were designed from within probe sequences represented on the microarrays, and quantitative reverse transcription (qRT)-PCR was used to quantify representative transcripts involved in ROS homeostasis. A total of 30 pairs of microarray and qRT-PCR data were obtained for wheat. A comparison of the wheat qRT-PCR results with the corresponding microarray data resulted in a correlation coefficient of 0.94 with $P = 8.3 \times 10^{-15}$ (Fig. 4A). A total of 33 pairs of microarray and qRT-PCR data were obtained for rice. A comparison of the rice qRT-PCR results with the corresponding microarray data resulted in a correlation coefficient of 0.95 with $P = 2.2 \times 10^{-16}$ (Fig. 4B).

qRT-PCR results for two wheat transcripts encoding class III peroxidases, CK198851 and CD373657, are shown in Figure 4, C and D. The transcript levels corresponding to CK198851 were the same as the control in resistant plants 12 h after Hessian fly attack began, peaked at 3.1-fold ($P = 5.0 \times 10^{-3}$) above the control at 24 h, and gradually returned to control levels by 120 h (Fig. 4C). The same samples were used for the microarray and qRT-PCR analyses, but the qRT-PCR

Table III. *Rice microarray changes in transcript abundance following Hessian fly larval attack*

Gene Category[a]	Total Probe Sets[b]	Abundance[c]	
		Increased	Decreased
Potential ROS generating	179	26	1
NADPH-dependent oxidases	8	1	0
Alternative oxidases	6	0	0
Glycolate oxidases	2	0	0
Oxalate oxidases	2	0	0
Amine oxidases	21	1	0
Class III peroxidases	133	23	1
Phospholipases A2	6	0	0
Xanthine dehydrogenases	1	1	0
Potential ROS scavenging	141	7	14
Catalases	3	1	0
Superoxide dismutases	9	0	2
Glutathione reductases	3	0	0
Dehydroascorbate reductase	2	0	0
Peroxiredoxins and thioredoxins	58	0	8
Glutaredoxins	26	1	0
Ferredoxins	14	0	1
Ascorbate peroxidases	12	0	3
Glutathione peroxidases	4	2	0
Flavanone 3-hydroxylases	10	3	0

[a]Gene category based on probe set annotation. [b]Number of probe sets on the Rice GeneChip microarray. [c]Transcript abundance level compared with levels in a nonattacked control plant at the 12-h time point, cumulative for all time points.

fold changes were about two times higher than those detected by the microarray, indicating that qRT-PCR was more sensitive at detecting this message. In susceptible plants, the abundance of this transcript decreased over time from the same level as in the control at 12 h to 9.0-fold ($P = 8.6 \times 10^{-5}$) below the control by 120 h after the initiation of attack (Fig. 4C). The transcript levels corresponding to CD373657 responded quickly in resistant wheat plants (Fig. 4D), being 4.9-fold above control levels ($P = 1.5 \times 10^{-5}$) 12 h after attack, reaching a maximum of 18.6-fold ($P = 5.2 \times 10^{-8}$) by 24 h, and returning to 2.3-fold ($P = 2.1 \times 10^{-3}$) by 120 h. In susceptible plants, transcript levels were similar to controls throughout the time course (Fig. 4D). Again, qRT-PCR data displayed larger fold changes than were detectable on the microarray, but the overall trends in transcript abundance were the same for both qRT-PCR and microarray data sets (Table II; Supplemental Table S1).

qRT-PCR results for the transcripts of two rice class III peroxidase genes, Os06g0547400 and Os07g0677200, are shown in Figure 4E. qRT-PCR detected a strong increase in the mRNA levels for these two genes, which was also observed in our microarray analysis (Table IV; Supplemental Table S1). In addition, qRT-PCR detected a sustained, moderate increase in the transcript of a rice NADPH-dependent oxidase gene, Os01g0734200, whereas a sustained, moderate decrease was detected in the transcript of a rice thioredoxin gene, Os04g0676100 (Fig. 4F), which were again in agreement with microarray data (Supplemental Table S1).

Hessian Fly-Induced Increase in Peroxidase Enzymatic Activity

Since class III peroxidase transcripts were the only group that increased commonly in both wheat and rice seedlings during incompatible and nonhost interactions, the enzymatic activity of peroxidases at the attack site was assayed using a technique (see "Materials and Methods") similar to that used to assay H_2O_2 (Fig. 5). No significant difference in peroxidase activity was detected between control and attacked wheat during compatible interactions (Fig. 5A, Newton). However, a 2-fold increase was detected in attacked plants during incompatible interactions with the resistant *H9* (Iris) and *H13* (Molly) wheat (Fig. 5). Rice seedlings were more sensitive to the assay, probably because a higher basic level of peroxidases resulted in brighter fluorescent images under the same conditions (Fig. 5A, Rice). Quantification of fold changes between control and attacked plants yielded similar results in nonhost rice seedlings and wheat seedlings during incompatible interactions (Fig. 5B).

DISCUSSION

In contrast to extensive evidence for a major role of ROS in plant defense against pathogens (Lamb and Dixon, 1997), evidence for a role of ROS in plant defense against insects is still preliminary, sporadic, and inconsistent (Giovanini et al., 2006; Moloi and van der Westhuizen, 2006; Chen, 2008). In this research, accumulation of ROS at the attack site in three isogenic

Table IV. *Changes in the abundance of transcripts potentially involved in ROS generation in rice*

Includes transcripts from rice plants fulfilling the following criterion: significant fold change of $P < 0.05$ in nonhost interactions compared with a nonattacked control. NC, No change.

Rice Gene Identifier[a]	Fold Change[b]		Net Increase[c]	
	24 h	72 h	24 h	72 h
NADPH oxidase[d]				
Os01g0734200	2.1	1.4	1,175.6	427.5
Amine oxidase[d]				
CB620528[e]	5.0	3.9	183.2	132.8
Xanthine dehydrogenase[d]				
Os03g04¯29800	1.3	NC	403.2	0
Class III peroxidase[d]				
Os07g0677200	21.5	6.0	1,246.4	304.6
Os01g0326300	13.5	10.8	60.0	47.0
Os06g0547400	4.3	2.5	853.3	381.5
Os12g0112000	8.8	5.3	2,622.9	1,456.9
Os04g0688500	15.4	5.5	87.8	27.5
Os04g0688200	6.7	3.9	292.4	148.8
Os01g0327400	3.2	3.1	3,263.0	3,114.7
Os01g0327100	2.4	3.8	321.6	643.2
Os06g0681600	1.7	1.8	974.8	1,114.1
BI812086[e]	1.5	1.3	20.3	12.2
Os02g0240100	1.9	NC	26.4	0
Os01g0963000	4.0	NC	88.5	0
D14482[e]	3.5	NC	184.8	0
Os07g0676900	2.8	NC	217.2	0
Os05g0135500	1.3	NC	1,203.3	0
Os04g0688100	5.4	NC	14,263.9	0
Os04g0688300	6.0	NC	3,611.5	0
Os07g0694300	2.7	NC	463.3	0
Os03g0339400	1.9	NC	580.4	0
Os05g0499400	1.7	NC	491.5	0
Os11g0210100	1.6	NC	2,743.6	0
Os05g0134400	1.3	NC	4,751.50	0

[a]Gene names corresponding to probe sequences on the RiceChip. [b]Fold change is based on values for the same probe sets in a nonattacked control plant at the 12-h time point. [c]Net increase in relative fluorescence level is based on values for the same probe sets at the 12-h time point in nonattacked control plants (SIC in Supplemental Table S1). Transcripts with the highest numbers are the most abundant. [d]Based on HarvEST and National Center for Biotechnology Information database searches. [e]Gene is not named.

wheat lines, Newton, Iris, and Molly, and the rice line Nipponbare was examined following Hessian fly infestation. Newton is the susceptible recurrent parent, whereas Iris and Molly carry *R* genes *H9* and *H13*, respectively (Patterson et al., 1994). *H9* and *H13*, located on different chromosomes (Liu et al., 2005a, 2005b), are both major dominant genes that have a gene-for-gene interaction with Hessian fly avirulence. Rice is a nonhost of Hessian fly (Chen et al., 2009b). A sustained accumulation of H_2O_2 was observed at the attack site in Iris and Molly as well as in Nipponbare but was not observed in Newton when attacked by Hessian fly larvae, indicating that ROS is likely part of a gene-for-gene defense in resistant wheat and nonhost defense in rice. It was impossible to determine how much ROS was ingested by Hessian fly larvae or the degree of toxicity, because of the inability to rear the larvae on artificial diet. However, a toxicity assay revealed that a small amount (LD50 $< 0.05\ \mu g\ mL^{-1}$ or 1.7 μM) of H_2O_2 in an artificial diet could cause the death of *Drosophila* larvae (Fig. 3). H_2O_2 concentrations in the incubation medium of plant cells undergoing an oxidative burst can reach 10 to 100 μM (Kauss and Jeblick, 1996; Bolwell et al., 1998; Küpper et al., 2001). These observations suggest that ROS could have a direct, detrimental effect on Hessian fly larvae. Consistent with this possibility, transcripts for genes encoding a range of antioxidant enzymes became more abundant in the guts of Hessian fly larvae that fed on resistant plants (Mittapalli et al., 2007). ROS are likely involved in plant defense against other galling insects, because plant hypersensitive symptoms have been observed during these interactions (Chen, 2008). In addition to ROS, other likely defense chemicals reported in the literature include lectins (Subramanyam et al., 2006), inhibitors of digestive enzymes (Wu et al., 2008), and secondary metabolites (Liu et al., 2007). A combination of toxic defense chemicals accumulated

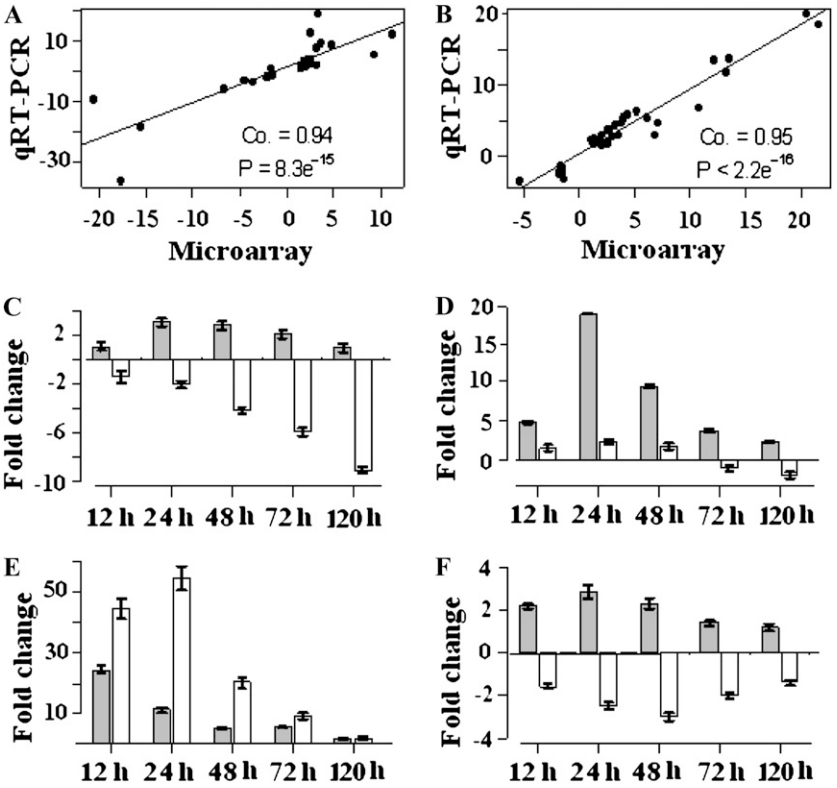

Figure 4. qRT-PCR validation of microarray data. A and B, Spearman's rank correlation between qRT-PCR and the corresponding microarray data for wheat transcripts (A) and rice transcripts (B). C, qRT-PCR quantification of the wheat class III peroxidase transcript CK198851. Graphs show fold change values for attacked resistant (gray bars) and susceptible (white bars) wheat plants at 12, 24, 48, 72, and 120 h post egg hatch when compared with nonattacked wheat plants at the same time point. D, qRT-PCR quantification of the wheat transcript CD373657 displayed like the data in C. E, qRT-PCR quantification of two rice class III peroxidase genes, Os06g0547400 (gray bars) and Os07g0677200 (white bars), showing fold change values for attacked rice plants at 12, 24, 48, 72, and 120 h after egg hatch compared with nonattacked control plants at the 12-h time point. F, qRT-PCR quantification of a rice NADPH-dependent oxidase gene (Os01g0734200; gray bars) and a thioredoxin gene (Os04g0676100; white bars) displayed like the data in C.

at the attack site is the likely cause for the death of Hessian fly larvae within resistant plants. Hessian fly larvae die in resistant and nonhost plants within 3 to 5 d without apparent growth and development (Anderson and Harris, 2006; Subramanyam et al., 2008; Chen et al., 2009b).

Even though the search for the source of ROS generation has been extensive, the mechanism responsible for the rapid accumulation of ROS is still open to question, and different plant-parasite systems may follow different pathways (Mika et al., 2004). Because de novo synthesis of proteins is needed to sustain the accumulation of ROS following pathogen attack or artificial elicitation (Lamb and Dixon, 1997; Grant and Loake, 2000), the transcripts with increased abundance specifically during incompatible interactions are candidates for ROS generation in resistant and nonhost plants. From a global analysis of changes in the levels of 129 unique wheat transcripts that are proposed to be involved in ROS generation, two groups of transcripts, one encoding oxalate oxidases and the other encoding class III peroxidases, showed significant net increases in wheat during incompatible interactions (Table II). Therefore, oxalate oxidases and class III peroxidases were potential sources for ROS production in attacked resistant wheat. A similar analysis of 179 rice transcripts potentially involved in ROS generation revealed increases in a NADPH oxidase, an amine oxidase, a xanthine dehydrogenase, and 26 class III peroxidase transcripts (Table IV).

Because both resistant wheat and nonhost rice exhibited an increased accumulation of a large number of class III peroxidase transcripts, this type of peroxidase may play a major role in ROS generation during attack by Hessian fly larvae. Enzymatic activity of peroxidases was elevated at the attack site of rice seedlings (Fig. 5). The increased peroxidase activity was likely contributed by class III peroxidases; this group of proteins is secretory, whereas other types of peroxidases are located in different compartments (Teixeira et al., 2006; Toppo et al., 2008). The increased enzymatic peroxidase activity at the attack site could provide the molecular basis for the enhanced generation of ROS. Class III (cell wall-associated) peroxidases are secreted into the apoplastic space and have been proposed as a producer of H_2O_2 (Kawano, 2003; Mika et al., 2004; Passardi et al., 2004b; Cosio and Dunand, 2009). The accumulation of H_2O_2 in some plants was cyanide sensitive and totally inhibited by the peroxidase inhibitor azide (Bolwell et al., 1995). In French bean cells, a transient alkalinization at the apoplastic space induced by an elicitor can activate a class III peroxidase, which can generate H_2O_2 in the presence of some reductants (Bolwell et al., 2002). When the counterpart of the bean peroxidase was antisense suppressed in Arabidopsis through transgenic plants, the oxidative burst was diminished in response to pathogens (Bindschedler et al., 2006). Similarly, when the pepper (*Capsicum annuum*) peroxidase gene *CaPO2* (class III) was silenced, the oxidative burst as well as

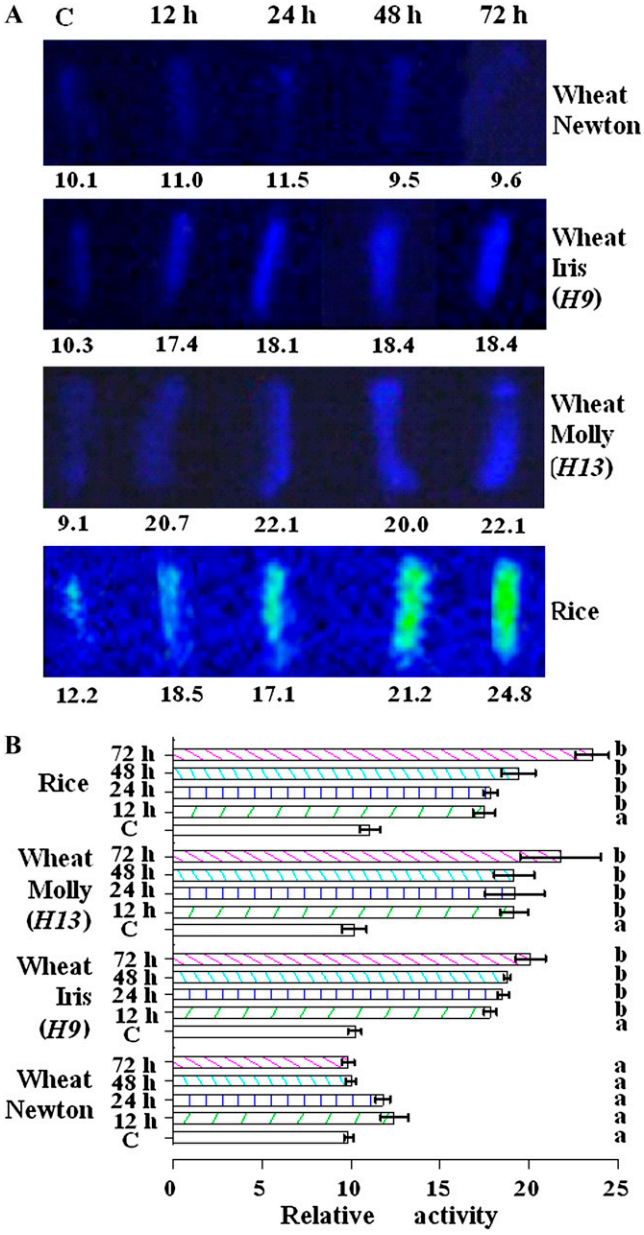

Figure 5. Changes in peroxidase activity at the attack site. A, Representative fluorescence images of leaf sheaths stained for peroxidase enzymatic activity. B, Average relative fluorescence obtained from three biological replicates. Materials and procedures were as described in Figure 1.

disease resistance were compromised (Choi et al., 2007). On the other hand, overexpression of the sweet potato (*Ipomoea batatas*) peroxidase gene *swpa4* resulted in increased H_2O_2 production and enhanced stress tolerance in tobacco (*Nicotiana tabacum*; Kim et al., 2008). Pairwise analysis revealed less than 45% sequence identity among the French bean, pepper, and sweet potato peroxidases (data not shown). Similar sequence identity also exists between the Hessian fly-induced wheat and rice peroxidases in comparison with the three H_2O_2-generating peroxidases from French bean, pepper, and sweet potato (Supplemental Fig. S1; data not shown). These lines of evidence suggest that a diversity of class III peroxidases may be able to produce H_2O_2 under certain conditions and that the Hessian fly-induced peroxidases may be responsible for elevated ROS production. It is also possible that some other types of unidentified genes participated in ROS production in plants attacked by Hessian fly larvae.

Consistent with the possibility that class III peroxidases were responsible for Hessian fly-induced ROS accumulation during incompatible and nonhost interactions, a much greater magnitude of increase (3- to 4-fold; Fig. 1B) in apoplastic H_2O_2 was observed in comparison with the increase (30%–40%; Fig. 2B) in cytosolic H_2O_2. Since there was no increase in the levels of transcripts of several genes known to be involved in cytosolic H_2O_2 production (Supplemental Table S1), the small increase in cytosolic H_2O_2 during incompatible and nonhost interactions was likely due to penetration of H_2O_2 from apoplasm into cytosol. H_2O_2 can penetrate cell membrane through water channels (Henzler and Steudle, 2000; Bienert et al., 2006). Alternatively, the slightly higher image intensity in resistant and nonhost plants could be due to a higher background of autofluorescence caused by other physiological factors such as a differences related to growth state (growth of resistant plants is inhibited initially and then accelerates after defense to compensate the initial growth deficit; Anderson and Harris, 2006).

The genetic relationship between wheat and rice genes that responded to Hessian fly attack was analyzed (Table V). Based on the first hit of BLASTx, 14 wheat transcripts that increased in abundance shared sequence similarity with rice class III peroxidase genes that also responded to Hessian fly attacks with increased transcript abundance. These class III peroxidase transcript levels increased in plants during both incompatible and nonhost interactions, but their levels were either not affected or decreased in plants during compatible interactions. These are candidate genes that may have participated in ROS generation in wheat and rice during attack by Hessian fly larvae. The class III peroxidase family consists of a large number of diversified genes in each plant species (http://peroxibase.toulouse.inra.fr/index.php). In rice, 138 class III peroxidase genes have been identified (Passardi et al., 2004a). There are likely many more peroxidase genes in wheat, since it has a much more complex genome. In our analysis, only 83 class III peroxidase transcripts were included. Therefore, it is almost certain that there are other peroxidase genes that were affected by Hessian fly attack but were not identified in our analysis. In addition to the potential role in ROS generation, class III peroxidases also perform critical functions in lignification, signaling, and various other processes (Cosio and Dunand, 2009). Enhanced cell wall lignification can fortify physical barriers and

Table V. *Genetic relationship between class III peroxidase sequences in wheat and rice*

All wheat and rice sequences shown became more abundant in attacked resistant/nonhost seedlings compared with nonattacked controls. Wheat sequences were either unaffected or decreased in abundance in attacked susceptible seedlings compared with nonattacked controls.

Wheat Sequence[a]	First-Hit Rice Sequence[a,b]	Sequence Similarity[b]		Highest Fold Change[c]	
		Identity	E Value	Wheat	Rice
CK196925	Os01g0963000	71%	2.00E-35	2.7	4.0
CK200808	Os04g0688100	60%	1.00E-06	12.1	5.4
BG606752	Os04g0688100	70%	7.00E-26	10.9	5.4
CA685359	Os04g0688100	33%	0.008	5.9	5.4
BJ284138	Os04g0688100	46%	1.00E-20	2.3	5.4
CA723231	Os04g0688100	61%	2.00E-16	2.2	5.4
CK195044	Os04g0688100	60%	6.00E-19	1.6	5.4
CD373657	Os04g0688200	75%	4.00E-65	3.4	6.7
CD373595	Os04g0688200	66%	1.00E-54	1.5	6.7
CA627644	Os06g0681600	69%	5.00E-15	1.4	1.8
CA661280	Os07g0677100	84%	1.00E-04	2.0	8.3
X85227	Os07g0677200	61%	4.00E-57	2.8	21.5
CA714005	Os07g0694300	74%	1.00E-08	1.4	2.8
CD373711	Os12g0112000	80%	5.00E-36	1.6	8.8

[a]GenBank accession numbers corresponding to probe set sequences from the WheatChip or RiceChip. [b]Based on BLAST analysis. [c]Fold change for wheat was calculated in comparison with nonattacked control samples taken at the same time point, whereas fold change for rice was calculated in comparison with nonattacked control samples taken at the 12-h time point.

increase indigestibility to attacking pests. Indeed, class III peroxidases have been linked to host resistance to a wide range of insects (Dowd and Lagrimini, 2006; Garcia-Lara et al., 2007) and pathogens (Choi et al., 2007; Johrde and Schweizer, 2008). It is possible that different mechanisms are deployed against different pests through activation of different class III peroxidases. Further research remains to be carried out on specific class III peroxidases and their biological implications.

The role of ROS in plant defense against insects other than Hessian fly remains to be determined. The feeding behavior of many gall midges shares similarity with plant pathogens, including a fixed feeding site, a requirement of live host plants, and secretion of effector proteins (Chen et al., 2004, 2008). A gene-for-gene interaction is also common to many plant-gall midge systems (Harris et al., 2003). Therefore, it is quite likely that plants use common defense mechanisms against gall midges and pathogens. ROS may also play a role in plant defense against aphids (Moloi and van der Westhuizen, 2006). Even though aphids can migrate from location to location, they need to invest major effort to establish a feeding site, including secretion of sheath proteins and suppression of wound responses (Miles, 1999). Consequently, aphids ingest food from a single location for a relatively long period, which provides the basis for the effectiveness of oxidative burst-type defense. Chewing insects usually exhibit greater mobility. The accumulation of ROS at the previous feeding site is not useful if the insect has migrated to another place. However, that does not exclude the effectiveness of ROS on other insects feeding nearby or the same insect when it returns.

The NADPH-dependent oxidase pathway, which is thought to be the main source for rapid generation of ROS during an oxidative burst in plants upon pathogen attack (Lamb and Dixon, 1997), was apparently not involved in ROS generation in wheat following Hessian fly attack. No increase was detected in the levels of transcripts encoding NADPH-dependent oxidases and superoxide dismutases in resistant wheat (Supplemental Table S1; Giovanini et al., 2006). One could argue that because the wheat microarray does not contain sequences for the entire transcriptome, one or more wheat NADPH-oxidase genes may not have been characterized and therefore were not included in the analysis. However, the rice genome is fully sequenced, and all of the rice NADPH oxidase genes were included in this study. Among the eight rice NADPH oxidase-like genes, only one showed increased transcript abundance after Hessian fly attack. The wheat homolog of this responsive rice gene was not affected by Hessian fly attack (Giovanini et al., 2006). In addition, diphenylene iodonium, an inhibitor of NADPH oxidases, did not have any effect on wheat seedlings in terms of their resistance to Hessian fly larvae (Giovanini et al., 2006).

The situation in rice appears to be different from that in wheat. As mentioned previously, levels of transcripts for one of the eight rice NADPH oxidase genes consistently increased after larval attack, as determined by both microarray and qRT-PCR (Fig. 4F; Supplemental Table S1). The level of superoxide increased 2- to 3-fold in Hessian fly-attacked rice, whereas the content of superoxide showed no statistically significant changes in resistant wheat attacked

by Hessian fly larvae (Fig. 1C). These results indicated that the rice NADPH-dependent oxidase may play a role in the generation of O_2^-.

In plant-pathogen interactions, the mRNA levels increase for plant genes encoding ROS-scavenging enzymes, and the higher levels of the encoded enzymes are thought to protect host cells from elevated ROS during oxidative bursts (Levine et al., 1994). The defense response was different during incompatible wheat-Hessian fly interactions; the majority of scavenger genes were not affected. For those affected genes, more transcripts decreased in abundance than increased (Table I; Supplemental Table S1). During compatible wheat-Hessian fly interactions, on the other hand, more transcripts encoding scavenger enzymes increased in abundance. In fact, the majority of the transcript levels examined was higher at the later time points (Table I; Supplemental Table S1). During nonhost rice-Hessian fly interactions, the levels of a few transcripts increased or decreased, but the abundance of the majority of the scavenger genes was not affected (Table III; Supplemental Table S1). Clearly, the situation is different between the plant-Hessian fly interaction and plant-pathogen interactions in terms of ROS-scavenger gene reactions. It is understandable that increased levels of scavenging enzymes will reduce the content of ROS and, therefore, reduce ROS toxicity to Hessian fly larvae during compatible interactions. During incompatible and nonhost interactions, the lack of increase in scavenger transcripts may reflect the fact that the class III peroxidases were secreted and, consequently, ROS species were produced extracellularly where there was no need to protect subcellular organelles from oxidative damage. Alternatively, the level of ROS accumulation during incompatible and nonhost interactions may not have been high enough to induce scavenger genes for cellular protection. The later possibility is unlikely, because Hessian fly attacks do induce hypersensitive lesion-like symptoms in a few wheat lines that contain *R* genes (Grover, 1995) and in rice (X.M. Liu and M.-S. Chen, unpublished data). The decrease in scavenger transcript abundance may also play a role in the increased accumulation of ROS by slowing down the degradation of ROS.

In conclusion, the wheat incompatible interaction and the nonhost response of rice share many characteristics and use similar genes in defense against Hessian fly, with some minor differences. Class III peroxidase genes appeared to be active in both types of defense. But NADPH oxidase transcript and superoxide levels increased only in rice, suggesting that the oxidative burst is a component of nonhost defense in the rice-Hessian fly interaction. Both defense responses against Hessian fly differed from pathogen defense in that ROS scavenger gene transcripts did not increase in abundance. In contrast, virulent Hessian fly larvae manipulated wheat defense genes to minimize the negative effects on their development.

MATERIALS AND METHODS

Hessian Fly Populations

Two Hessian fly (*Mayetiola destructor*) populations were used in this study: a Kansas population and biotype L. Biotype L was derived from a colony collected in Posey County, Indiana, in 1986 (Sosa and Gallun, 1973). The majority of the Kansas population is biotype GP, but it also contains insects virulent to several known wheat (*Triticum aestivum*) *R* genes (Chen et al., 2009a). Both biotype L and the Kansas population are virulent to Newton but avirulent to wheat lines Iris and Molly and to rice (*Oryza sativa*).

Plant Materials and Sample Collection

Three near-isogenic wheat lines, Iris (*H9*; resistant to biotype L; incompatible interaction), Molly (*H13*; resistant to biotype L; incompatible interaction), and Newton (susceptible to biotype L; compatible interaction), were planted in groups of 15 seeds per 4-inch pot containing Promix Professional growing medium (Premier Horticulture). Plants were maintained in a growth chamber at 18°C and a 24-h photoperiod with light intensity of 1,000 μmol m^{-2} s^{-1}. Seedlings at the one-leaf stage were infested with five mated female biotype L flies to achieve an infestation level of approximately 18 larvae per plant. The experiment consisted of three independent biological replicates. Each replicate included time series tissue samples from resistant, susceptible, and nonattacked control plants. Samples were harvested 12 h as well as 1, 2, 3, 5, and 8 d after egg hatch. For microarray experiments, four time point samples were used (1, 3, 5, and 8 d after egg hatch). For qRT-PCR, five time point samples were used (12 h plus 1, 2, 3, and 5 d after egg hatch). Each sample included crown tissue (a 2-cm piece above the root-shoot junction) from leaf 2, harvested from 32 to 40 plants. Harvested tissue was immediately frozen in liquid nitrogen.

Rice line Nipponbare, from which the rice genome was sequenced, was used in this study as a nonhost. Rice seeds were provided by the Dale Bumpers National Rice Research Center at Stuttgart, Arkansas. Rice seedlings were germinated in petri dishes at 37°C. After germination, seeds with young plants were transplanted to soil in individual pots and grown in a growth chamber set at 30°C (day)/28°C (night) with a 14-h/10-h (light/dark) photoperiod until plants reached the 2.5-leaf stage (when the third leaf begins to emerge from the whorl). Because the first leaf of rice is very small, the 2.5-leaf stage of rice seedlings is essentially equivalent to the 1.5-leaf stage of wheat seedlings. Rice seedlings were infested with one female per plant, which is three times the level for wheat infestation. The increased number of females was necessary to achieve an infestation level similar to wheat, since larvae enter the whorl of rice plants with a lower success rate. The rice plants were maintained in a growth chamber set at 20°C ± 1°C (day) and 18°C ± 1°C (night) with a 14-h/10-h (light/dark) photoperiod. Sample collection was as described in wheat except that crown tissue from the third leaf was collected.

Determination of Relative H_2O_2 Concentration

Two different approaches were adapted to determine apoplastic and cytosolic H_2O_2. An uptake assay was conducted to determine the relative concentration of apoplastic H_2O_2 using the Amplex Red Hydrogen Peroxide/Peroxidase Assay Kit (Molecular Probes/Invitrogen). In this assay, apoplastic H_2O_2 reacts with the chemical 10-acetyl-3,7-dihydroxyphenoxazine to produce the red-fluorescent oxidation product resorufin in a 1:1 stoichiometry in the presence of saturated horseradish peroxidase. Therefore, an increase in fluorescence in attacked plants in comparison with nonattacked plants gives an estimation of changes in the relative levels of apoplastic H_2O_2. Fresh leaf sheaths (approximately 1.5 cm length) at the attack site of infested plants (defined for wheat and rice above) were collected at 12, 24, 48, and 72 h after the initial Hessian fly attack. The corresponding leaf sheaths of nonattacked plants were taken as controls. For each assay, four leaf sheaths were placed together on a microscope slide. The leaf sheaths were then soaked in 500 μL of the Amplex Red reagent containing horseradish peroxidase for 30 min with protection from light. Luminescence emission signals (images) were detected and captured with a liquid nitrogen-cooled CCD camera coupled to the microscope and an ST-133 Controller (Princeton Instruments; Zhang et al., 2007). The relative content of H_2O_2 was calculated with Winview Imaging software (Roper Scientific). Each treatment was repeated three times.

A penetration assay was conducted to determine the relative concentration of cytosolic H_2O_2 using the Image-iT Live Green ROS Detection Kit (Molecular Probes/Invitrogen; Yoshiyuki et al., 2001). In this assay, the chemical 5-(and-

6)-carboxy-2′,7′-dichlorodihydrofluorescin diacetate is nonfluorescent and can permeate live cells. After penetrating into a cell, 2′,7′-dichlorodihydrofluorescin diacetate is converted by intracellular esterases to an impermeable chemical called carboxy-dichlorodihydrofluorescein, which is further oxidized by H_2O_2. The oxidized carboxy-dichlorodihydrofluorescein emits green fluorescence at 529 nm. Thin epidermal tissues were obtained with a razor blade from leaf sheaths at the feeding site where larvae were located. The tissues were washed five times with Hank's balanced salt buffer solution (Gibco 14025-092) to remove enzymes and other cellular components from broken cells and then stained following the protocol provided by the manufacturer. The stained tissues were examined with a fluorescent microscope (Zeiss Axioplan-2; 10 × 63) equipped with the appropriate filter set. Images were acquired with a digital camera under the same settings, and the luminosity of fluorescence emission was analyzed using Adobe Photoshop 6.0.

Determination of Enzymatic Activity of Peroxidases

The enzymatic activity of peroxidases was determined following the same procedure as the determination of H_2O_2 except that the Amplex Red reagent contained 2 mM H_2O_2 instead of horseradish peroxidase.

Determination of Superoxide

O_2^- was determined with a LumiMax Superoxide Anion Detection Kit (Stratagene) following the protocol provided by the manufacturer. The procedure is essentially the same as the determination of H_2O_2 described previously except that the leaf sheaths were soaked in a superoxide anion assay reagent for 60 min before image development.

Toxicity Assay

A *Drosophila melanogaster* colony was kindly provided by Dr. Yoonseong Park at the Department of Entomology, Kansas State University. The colony was maintained in Jazz-mix *Drosophila* medium (AS-153; Fisher). To synchronize larvae for the bioassay, about 200 adult flies were transported into a polyethylene rearing bottle (57 mm long × 57 mm wide; AS-359; Fisher) with fresh medium for egg deposition for 16 h. The adults were then removed from the bottle, and the eggs were incubated at room temperature. After 24 h, the medium was dissolved into a 15% Suc solution. Under this condition, larval insects floated whereas the residue of food sank to the bottom. The larvae were washed twice by transferring into a new bottle containing fresh Suc solution, each time using a P1000 pipet tip. For toxicity assay, individual larvae were transferred by pipet tip into a 1.5-mL microfuge tube that contained fresh *Drosophila* medium. Excess Suc solution transferred along with the larva was absorbed and removed with a paper tissue. Different concentrations of H_2O_2 (0.001, 0.005, 0.01, 0.05, 0.1, 0.2, and 0.3 μg mL^{-1}) were incorporated into the medium within a tube before the larval transfer. The mortality rate was determined after 1 week, when the larvae had either died or pupated. Ten larvae were tested for each H_2O_2 concentration for each replicate. Each test was repeated three times. Ten larvae were reared in medium containing no H_2O_2 at the same time for each replicate and were used as controls.

Microarray Hybridization and Analysis

The GeneChip Wheat Genome Array (Affymetrix) was used for wheat microarray studies. RNA was isolated from frozen tissue with TRIzol reagent (Invitrogen) according to the manufacturer's instructions. Generation of copy RNA, fluorescent labeling, hybridization, scanning, and quantification of hybridized Affymetrix wheat arrays was performed according to the Affymetrix GeneChip Expression Analysis Technical Manual at the Purdue University Genomics Core Facility.

Normalization of the microarray data was achieved using the Robust Multichip Average method (Irizarry et al., 2003; Gautier et al., 2004). The raw *P* values for simple comparisons were calculated in the computer language R (http://www.R-project.org) and analyzed using ANOVA in the Bioconductor package Limma (Smyth, 2005).

With treatment (infested or uninfested) as the factor, a linear model was fitted for each combination of plant type, time point, and probe set. An empirical Bayes approach was used to moderate *t* statistics. The raw *P* values were adjusted for multiple testing to control the false discovery rate (Benjamini and Hochberg, 1995). False discovery rate = 0.05 was set as the cutoff for statistical significance. Reported mRNA fold changes were calculated by comparing mRNA abundance levels for each infested treatment sample with the mRNA abundance in nonattacked control samples at the same time point.

Probe sets annotating to genes involved in generating and scavenging ROS were initially selected according to Affymetrix (http://www.affymetrix.com/index.affx) and then confirmed through HarvEST software (http://harvest.ucr.edu; Wheat 1 Array, version 1.53) and/or the National Center for Biotechnology Information BLAST software (http://blast.ncbi.nlm.nih.gov/Blast.cgi).

The Affymetrix GeneChip Rice Genome Array was used for rice gene expression studies. Hybridization and bioinformatics analysis were carried out following the same procedures as described for wheat. However, all experiments with rice were conducted in the Integrated Genomics Facility at Kansas State University. Rice samples for microarray analyses were collected at 12, 24, 48, and 72 h after initial Hessian fly attack. Data from infested samples were normalized using the same nonattacked control collected at 12 h.

qRT-PCR Analysis

DNase-treated RNA was the template for cDNA synthesis using random hexamers with the Tetro cDNA synthesis kit (Bioline) according to the manufacturer's guidelines. Samples were then treated with RNase H (Invitrogen). cDNA was quantified on a Nanodrop ND-1000 (NanoDrop Technologies) spectrophotometer, and samples were diluted to 15 ng μL^{-1} to ensure equal amounts of cDNA template for quantification of mRNA abundance.

qRT-PCR for selected wheat genes was conducted on an ABI PRISM Fast 7500 Sequence Detector at the Purdue University campus with the SYBR Green I dye-based detection system (Applied Biosystems) as described previously (Subramanyam et al., 2006) with slight modifications; a final reaction volume of 10 μL was subjected to PCR using the following parameters: 95°C for 10 min, then 40 cycles of 95°C for 3 s and 60°C for 30 s. A total of 10 representative Affymetrix target sequences exhibiting statistically significant fold changes were selected for analysis. Target-specific primers (Supplemental Table S2) were designed using Primer Express Software version 1.5 (Applied Biosystems). mRNA abundance of the gene encoding 60S ribosomal protein L21 (*RPL21*) was used as an endogenous control in qRT-PCR.

Quantification of mRNA levels detected by qRT-PCR was based on the Relative Standard Curve method (User Bulletin 2; ABI). Statistical significance for the log-transformed arbitrary expression values (Puthoff et al., 2005) was analyzed by ANOVA using the PROCMIXED procedure of SAS (SAS Institute SAS/STAT User's Guide, version 9.13). The ANOVA model included treatment, time points, and their interaction. Data from three biological replicates (each replicate assayed two times in independent qRT-PCR experiments) were combined and included as a random effect in the analysis. Fold change calculations were performed by comparing mRNA abundance of selected genes in infested plants with mRNA abundance levels for the same genes in nonattacked control samples that were collected simultaneously at the same time points as the infested samples. Fold change was considered statistically significant if the *P* value was <0.05.

qRT-PCR for selected rice genes was performed at the Kansas State University campus with iQ SYBR Green Supermix on an iCycler real-time detection system (Bio-Rad Laboratories) according to the manufacturer's instructions. PCR primers and gene targets are listed in Supplemental Table S2. PCR programs and data analysis were conducted as described by Maddur et al. (2006).

Statistical Analysis

Data for H_2O_2, O_2^-, and peroxidase activity were modeled using ANOVA with plant type and time point as two factors. Differences were highly significant for the effect of the host-over-time interaction, with $P = 9.9 \times 10^{-10}$ for H_2O_2, 8.7×10^{-9} for O_2^-, and 2.3×10^{-6} for peroxidase activity. Tukey's pairwise comparisons based on Student's range statistics were then conducted. Tukey's 95% simultaneous confidence intervals for all pairwise comparisons were used to separate hosts at different times into groups with significant differences.

Spearman's rank correlations between qRT-PCR results and the corresponding microarray data were calculated to compare the consistency of the results.

Toxicity of H_2O_2 to *Drosophila* larvae was analyzed using logistic regression. The numbers of dead larvae were modeled using binomial distribution. The log odds of the probability of dead versus live were fitted as a linear function of the H_2O_2 concentrations. Differences among replicates for each concentration

were insignificant ($P = 0.468$), whereas differences among treatments with different concentrations were highly significant ($P = 2.5 \times 10^{-6}$). Accordingly, data from replicates with the same concentration were pooled to fit a final logistic model. The concentration effects remained highly significant, with $P < 2 \times 10^{-16}$. The percentage of death at each concentration and their lower and upper confidence limits were calculated from the fitted logistic model.

Supplemental Data

The following materials are available in the online version of this article.

Supplemental Figure S1. Sequence alignment of class III peroxidases from different types of plants.

Supplemental Table S1. Microarray data of transcripts involved in ROS homeostasis.

Supplemental Table S2. Gene-specific qRT-PCR primers.

ACKNOWLEDGMENTS

We thank Drs. Xiaoyan Tang at Kansas State University and John Fellers at the U.S. Department of Agriculture-Agricultural Research Service for reviewing an earlier version of the manuscript. We also thank Dr. Tang for providing equipment and expertise for the assays of ROS and hydrogen peroxidases.

Received November 6, 2009; accepted December 1, 2009; published December 4, 2009.

LITERATURE CITED

Anderson KG, Harris MO (2006) Does R gene resistance allow wheat to prevent plant growth effects associated with Hessian fly (Diptera: Cecidomyiidae) attack? J Econ Entomol **99:** 1842–1853

Apel K, Hirt H (2004) Reactive oxygen species: metabolism, oxidative stress, and signal transduction. Annu Rev Plant Biol **55:** 373–399

Asada K, Takahashi M (1987) Production and scavenging of active oxygen in photosynthesis. *In* DJ Kyle, CB Osmond, CJ Amtzen, eds, Photoinhibition (Topics in Photosynthesis), Vol 9. Elsevier, Amsterdam, pp 227–287

Benjamini Y, Hochberg Y (1995) Controlling the false discovery rate: a practical and powerful approach to multiple testing. J R Stat Soc B **57:** 289–300

Bentur JS, Kalode MB (1996) Hypersensitive reaction and induced resistance in rice against the Asian rice gall midge Orseolia oryzae. Entomol Exp Appl **78:** 77–81

Bienert G, Schjoerring JK, Jahn TP (2006) Membrane transport of hydrogen peroxide. Biochim Biophys Acta **1758:** 994–1003

Bindschedler LV, Dewdney J, Blee KA, Stone JM, Asai T, Plotnikov J, Denoux C, Hayes T, Gerrish C, Davies DR, et al (2006) Peroxidase-dependent apoplastic oxidative burst in Arabidopsis required for pathogen resistance. Plant J **47:** 851–863

Bolwell GP, Bindschedler LV, Blee KA, Butt V, Davies DR, Gardner SL, Gerrish C, Minibayeva F (2002) The apoplastic oxidative burst in response to biotic stress in plants: a three-component system. J Exp Bot **53:** 1367–1376

Bolwell GP, Butt V, Davies DR, Zimmerlin A (1995) The origin of the oxidative burst in plants. Free Radic Res **23:** 517–532

Bolwell GP, Davies DR, Gerrish C, Auh CK, Murphy TM (1998) Comparative biochemistry of the oxidative burst produced by rose and French bean cells reveals two distinct mechanisms. Plant Physiol **116:** 1379–1385

Chen MS (2008) Inducible direct plant defense against insect herbivores: a review. Insect Sci **15:** 101–114

Chen MS, Echegaray E, Whitworth RJ, Wang H, Sloderbeck PE, Knutson A, Giles KL (2009a) Virulence analysis of Hessian fly (*Mayetiola destructor*) populations from Texas, Oklahoma, and Kansas. J Econ Entomol **102:** 774–780

Chen MS, Fellers JP, Stuart JJ, Reese JC, Liu XM (2004) A group of related cDNAs encoding secreted proteins from Hessian fly [*Mayetiola destructor* (Say)] salivary glands. Insect Mol Biol **13:** 101–108

Chen MS, Liu XM, Wang H, El Bouhssini M (2009b) Hessian fly (*Mayetiola destructor*) interactions with barley, rice, and wheat seedlings. J Econ Entomol **102:** 1663–1672

Chen MS, Zhao HX, Zhu YC, Scheffler B, Liu XM, Liu X, Hulbert S, Stuart JJ (2008) Analysis of transcripts and proteins expressed in the salivary glands of Hessian fly (*Mayetiola destructor*) larvae. J Insect Physiol **54:** 1–16

Choi HW, Kim YJ, Lee SC, Hong JK, Hwang BK (2007) Hydrogen peroxide generation by the pepper extracellular peroxidase CaPO2 activates local and systemic cell death and defense response to bacterial pathogens. Plant Physiol **145:** 890–904

Cosio C, Dunand C (2009) Specific functions of individual class III peroxidase genes. J Exp Bot **60:** 391–408

Dat J, Vandenabeele S, Vranova E, Van Montagu M, Inze D, Van Breusegem F (2000) Dual action of the active oxygen species during plant stress responses. Cell Mol Life Sci **57:** 779–795

Dowd PF, Lagrimini LM (2006) Examination of the biological effects of high anionic peroxidase production in tobacco plants grown under field conditions. I. Insect pest damage. Transgenic Res **15:** 197–204

Flor HH (1946) Genetics of pathogenicity in *Melamspora lini*. J Agric Res **73:** 335–357

Garcia-Brugger A, Lamotte O, Vandelle E, Bourque S, Lecourieux D, Poinssot B, Wendehenne D, Pugin A (2006) Early signaling events induced by elicitors of plant defenses. Mol Plant Microbe Interact **19:** 711–724

Garcia-Lara S, Arnason JT, Diaz-Pontones D, Gonzalez E, Bergvinson DJ (2007) Soluble peroxidase activity in maize endosperm associated with maize weevil resistance. Crop Sci **47:** 1125–1130

Garza R, Vera J, Cardona C, Barcenas N, Singh SP (2001) Hypersensitive response of beans to *Apion godmani* (Coleoptera: Curculionidae). J Econ Entomol **94:** 958–962

Gautier L, Cope L, Bolstad BM, Irizarry RA (2004) Analysis of Affymetrix GeneChip data at the probe level. Bioinformatics **20:** 307–315

Gechev TS, Breusegem FV, Stone JM, Denev I, Loloi C (2006) Reactive oxygen species as signals that modulate plant stress responses and programmed cell death. Bioessays **28:** 1091–1101

Giovanini MP, Puthoff DP, Nemacheck JA, Mittapalli O, Saltzmann KD, Ohm HW, Shukle RH, Williams CE (2006) Gene-for-gene defense of wheat against the Hessian fly lacks a classical oxidative burst. Mol Plant Microbe Interact **19:** 1023–1033

Giovanini MP, Saltzmann KD, Puthoff DP, Gonzalo M, Ohm HW, Williams CE (2007) A novel wheat gene encoding a putative chitin-binding lectin is associated with resistance against Hessian fly. Mol Plant Pathol **8:** 69–82

Grant JJ, Loake GJ (2000) Role of reactive oxygen intermediates and cognate redox signaling in disease resistance. Plant Physiol **124:** 21–29

Grover PBJ (1995) Hypersensitive response of wheat to Hessian fly. Entomol Exp Appl **74:** 283–294

Harris MO, Freeman TP, Rohfritsch O, Anderson KG, Payne SA, Moore JA (2006) Virulent Hessian fly (Diptera: Cecidomyiidae) larvae induce a nutritive tissue during compatible interactions with wheat. Ann Entomol Soc Am **99:** 305–316

Harris MO, Sandanayaka M, Griffin W (2001) Oviposition preferences of the Hessian fly and their consequences for the survival and reproductive potential of offspring. Ecol Entomol **26:** 473–486

Harris MO, Stuart JJ, Mohan M, Nair S, Lamb RJ, Rohfritsch O (2003) Grasses and gall midges: plant defense and insect adaptation. Annu Rev Entomol **48:** 549–577

Heath MC (2000) Hypersensitive response-related death. Plant Mol Biol **44:** 321–334

Henzler T, Steudle E (2000) Transport and metabolic degradation of hydrogen peroxide in *Chara coralline:* model calculations and measurements with the pressure probe suggest transport of H_2O_2 across water channels. J Exp Bot **51:** 2053–2066

Hoglund S, Larrson S, Wingsle G (2005) Both hypersensitive and non-hypersensitive responses are associated with resistance in *Salix viminalis* against the gall midge *Dasineura marginemtorquens*. J Exp Bot **56:** 3215–3222

Hu X, Bidney DL, Yalpani N, Duvick JP, Crasta O, Folkerts O, Lu G (2003) Overexpression of a gene encoding hydrogen peroxide-generating oxalate oxidase evokes defense responses in sunflower. Plant Physiol **133:** 170–181

Irizarry RA, Hobbs B, Collin F, Beazer-Barclay YD, Antonellis KJ, Scherf

U, Speed TP (2003) Exploration, normalization, and summaries of high-density oligonucleotide array probe level data. Biostatistics **4:** 249–264

Johrde A, Schweizer P (2008) A class III peroxidase specifically expressed in pathogen-attacked barley epidermis contributes to basal resistance. Mol Plant Pathol **9:** 687–696

Kauss H, Jeblick W (1996) Influence of salicylic acid on the induction of competence for H_2O_2 elicitation. Plant Physiol **111:** 755–763

Kawano T (2003) Roles of the reactive oxygen species-generating peroxidase reactions in plant defense and growth induction. Plant Cell Rep **21:** 829–837

Kim YH, Kim CY, Song WK, Park DS, Kwon SY, Lee HS, Bang JW, Kwak SS (2008) Overexpression of sweetpotato *swpa4* peroxidase results in increased hydrogen peroxide production and enhances stress tolerance in tobacco. Planta **227:** 867–881

Küpper FC, Kloareg B, Guern J, Potin P (2001) Oligoguluronates elicit an oxidative burst in the brown algal kelp *Laminaria digitata*. Plant Physiol **125:** 278–291

Lamb C, Dixon RA (1997) The oxidative burst in plant disease resistance. Annu Rev Plant Physiol Plant Mol Biol **48:** 251–275

Levine A, Tenhaken R, Dixon R, Lamb C (1994) H_2O_2 from the oxidative burst orchestrates the plant hypersensitive disease response. Cell **79:** 583–593

Liu XL, Bai J, Huang L, Zhu L, Liu X, Weng N, Reese JC, Harris M, Stuart JJ, Chen MS (2007) Gene expression of different wheat genotypes during attack by virulent and avirulent Hessian fly (*Mayetiola destructor*) larvae. J Chem Ecol **33:** 2171–2194

Liu XM, Fritz AK, Reese JC, Wilde GE, Gill BS, Chen MS (2005a) *H9, H10,* and *H11* compose a cluster of Hessian fly-resistance genes in the distal gene-rich region of wheat chromosome 1AS. Theor Appl Genet **110:** 1473–1480

Liu XM, Gill BS, Chen MS (2005b) Hessian fly resistance gene *H13* is mapped to a distal cluster of *R* genes in chromosome 6DS of wheat. Theor Appl Genet **111:** 243–249

Maddur AA, Liu XM, Zhu YC, Fellers FP, Oppert B, Park YS, Bai J, Wilde GE, Chen MS (2006) Cloning and characterization of protease inhibitor-like cDNAs from the Hessian fly *Mayetiola destructor* (Say). Insect Mol Biol **15:** 485–496

Mika A, Minibayeva F, Beckett R, Luthje S (2004) Possible functions of extracellular peroxidases in stress-induced generation and detoxification of active oxygen species. Phytochem Rev **3:** 173–193

Miles PW (1999) Aphid saliva. Biol Rev Camb Philos Soc **74:** 41–85

Mittapalli O, Neal JJ, Shukle RH (2007) Antioxidant defense response in a galling insect. Proc Natl Acad Sci USA **104:** 1889–1894

Mittler R, Vanderauwera S, Gollery M, Breusegem FV (2004) Reactive oxygen gene network of plants. Trends Plant Sci **9:** 490–498

Moloi MJ, van der Westhuizen A (2006) The reactive oxygen species are involved in resistance response of wheat to the Russian wheat aphid. J Plant Physiol **163:** 1118–1125

Passardi F, Longet D, Penel C, Dunand C (2004a) The class III peroxidase multigenic family in rice and its evolution in land plants. Phytochemistry **65:** 1879–1893

Passardi F, Penel C, Dunand C (2004b) Performing the paradoxical: how plant peroxidases modify the cell wall. Trends Plant Sci **9:** 534–540

Patterson FL, Mass FB III, Foster JE, Ratcliffe RH, Cambron S, Safranski G, Taylor PL, Ohm HW (1994) Registration of eight Hessian fly resistant common winter wheat germplasm lines (Carol, Erin, Flynn, Iris, Joy, Karen, Lola, and Molly). Crop Sci **34:** 315–316

Puthoff DP, Sardesai N, Subramanyam S, Nemacheck JA, Williams CE (2005) *Hfr-2*, a wheat cytolytic toxin-like gene, is up-regulated by virulent Hessian fly larvae and feeding. Mol Plant Pathol **6:** 411–423

Razem FA, Bernards MA (2003) Reactive oxygen species production in association with suberization: evidence for an NADPH-dependent oxidase. J Exp Bot **54:** 935–941

Sagi M, Fluhr R (2001) Superoxide production by plant homologues of the $gp91^{phox}$ NADPH oxidase: modulation of activity by calcium and by tobacco mosaic virus infection. Plant Physiol **126:** 1281–1290

Saltzmann KD, Giovanini MP, Ohm HW, Williams CE (2010) Transcript profiles of two wheat lipid transfer protein-encoding genes are altered during attack by Hessian fly larvae. Plant Physiol Biochem **48:** 54–61

Saltzmann KD, Giovanini MP, Zheng C, Williams CE (2008) Virulent Hessian fly larvae manipulate the free amino acid content of host wheat plants. J Chem Ecol **34:** 1401–1410

Sardesai N, Subramanyam S, Nemacheck JA, Williams CE (2005) Modulation of defense-response gene expression in wheat during Hessian fly larval feeding. J Plant Interact **1:** 39–50

Sauge MH, Kervella J, Pascal T (1998) Settling behaviour and reproductive potential of the green peach aphid *Myzus persicae* on peach varieties and a related wild *Prunus*. Entomol Exp Appl **89:** 233–242

Smyth GK (2005) Limma: linear models for microarray data. *In* R Gentleman, V Carey, W Huber, R Irizarry, S Dudoit, eds, Bioinformatics and Computational Biology Solutions using R and Bioconductor. Springer, New York, pp 397–420

Sosa O, Gallun RL (1973) Purification of races B and C of the Hessian fly by genetic manipulation. Ann Entomol Soc Am **66:** 1065–1070

Stuart JJ, Chen MS, Harris MO (2008) Hessian fly. *In* C Kole, W Hunter, eds, Genome Mapping and Genomics in Animals, Vol 4. Springer, Berlin, pp 93–102

Subramanyam S, Sardesai N, Puthoff DP, Meyer JM, Nemacheck JA, Gonzalo M, Williams CE (2006) Expression of two wheat defense-response genes, *Hfr-1* and *Wci-1*, under biotic and abiotic stresses. Plant Sci **170:** 90–103

Subramanyam S, Smith DF, Clemens JC, Webb MA, Sardesai N, Williams CE (2008) Functional characterization of HFR1, a high-mannose N-glycan-specific wheat lectin induced by Hessian fly larvae. Plant Physiol **147:** 1412–1426

Teixeira FK, Menezes-Benavente L, Galvão VC, Margis R, Margis-Pinheiro L (2006) Rice ascorbate peroxidase gene family encodes functionally diverse isoforms localized in different subcellular compartments. Planta **224:** 300–314

Toppo S, Vanin S, Bosello V, Tosatto SCE (2008) Evolutionary and structural insights into the multifaceted glutathione peroxidase (Gpx) superfamily. Antioxid Redox Signal **10:** 1501–1514

Torres MA, Dangl JL, Jones JDG (2002) *Arabidopsis* $gp91^{phox}$ homologues *AtrbohD* and *AtrbohF* are required for accumulation of reactive oxygen intermediates in the plant defense response. Proc Natl Acad Sci USA **99:** 517–522

Walters DR (2003) Polyamines and plant disease. Phytochemistry **64:** 97–107

Williams CE, Collier CC, Nemacheck J, Liang C, Cambron SE (2002) A lectin-like wheat gene responds systemically to attempted feeding by avirulent first-instar Hessian fly larvae. J Chem Ecol **28:** 1411–1428

Wojtaszek P (1997) Mechanisms for the generation of reactive oxygen species in plant defense response. Acta Physiol Plant **19:** 581–589

Wu JX, Liu XM, Zhang SZ, Zhu YC, Whitworth RJ, Chen MS (2008) Differential responses of wheat inhibitor-like genes to Hessian fly, *Mayetiola destructor*, attacks during compatible and incompatible interactions. J Chem Ecol **34:** 1005–1012

Yoshiyuki N, Pei ZM, Mori IC, Schroeder J (2001) Abscisic acid activation of plasma membrane Ca^{2+} channels in guard cells requires cytosolic NAD(P)H and is differentially disrupted upstream and downstream of reactive oxygen species production in *abi1-1* and *abi2-1* protein phosphatase 2C mutants. Plant Cell **13:** 2513–2523

Zeiss MR, Brandenburg RL, van Duyn JW (1993) Suitability of seven grass weeds as Hessian fly (Diptera: Cecidomyiidae) hosts. J Agric Entomol **10:** 107–119

Zhang J, Shao F, Li Y, Cui H, Chen L, Li H, Zou Y, Long C, Lan L, Chai J, et al (2007) A *Pseudomonas syringae* effector inactivates MAPKs to suppress PAMP-induced immunity. Cell Host Microbe **1:** 175–185

Zhu L, Liu XM, Liu X, Jeannotte R, Reese JC, Harris M, Stuart JJ, Chen MS (2008) Hessian fly (*Mayetiola destructor*) attack causes dramatic shift in carbon and nitrogen metabolism in wheat. Mol Plant Microbe Interact **21:** 70–78